Influence of partial accommodation coefficients on the aerodynamic parameters of an airfoil in hypersonic, rarefied flow

Gennaro Zuppardi[*]

*Department of Industrial Engineering, University of Naples "Federico II",
Piazzale Tecchio 80, 80125 Naples, Italy*

Abstract.   The present paper is the follow-on of a former work in which the influence of the gas-surface interaction models was evaluated on the aerodynamic coefficients of an aero-space-plane and on a section of its wing. The models by Maxwell and by Cercignani-Lampis-Lord were compared by means of Direct Simulation Monte Carlo (DSMC) codes. In that paper the diffusive, fully accommodated, semi-specular and specular accommodation coefficients were considered. The results pointed out that the influence of the interaction models, considering the above mentioned accommodation coefficients, is pretty strong while the Cercignani-Lampis-Lord and the Maxwell models are practically equivalent. In the present paper, the comparison of the same models is carried out considering the dependence of the accommodation coefficients on the angle of incidence (or partial accommodation coefficients). More specifically, the normal and the tangential momentum partial accommodation coefficients, obtained experimentally by Knetchel and Pitts, have been implemented. Computer tests on a NACA-0012 airfoil have been carried out by the DSMC code DS2V-64 bits. The airfoil, of 2 m chord, has been tested both in clean and flapped configurations. The simulated conditions were those at an altitude of 100 km where the airfoil is in transitional regime. The results confirmed that the two interaction models are practically equivalent and verified that the use of the Knetchel and Pitts coefficients involves results very close to those computed considering a diffusive, fully accommodated interaction both in clean and flapped configurations.

Keywords: gas-surface interaction models; partial accommodation coefficients; direct simulation Monte Carlo method; airfoil aerodynamic coefficients in hypersonic, rarefied regime

1. Introduction

An accurate computation of the aerodynamic forces and moments of a space vehicle, in rarefied flow, is necessary for a correct design of the propulsion apparatus, of the systems controlling attitude and stability and of the systems facilitating maneuverability. The correct computation of forces and moments relies, in turn, on a proper choice of the gas-surface interaction model. This influences the computation of momentum and energy exchanged with the surface, therefore of the aerodynamic forces, moments and heat flux.

∗Corresponding author, Lecturer, E-mail: zuppardi@unina.it

It is well known that, in rarefied flow, the gas–surface interaction is considered as made of two separate steps: incidence and re-emission of the molecules. While the calculation of incidence step is proved to be accurate, the computation of the re-emission step is still today controversial. For this reason, many models were developed: Maxwell (Bird 1998, 2013), (Shen 2005), Cercignani-Lampis (Bird, 1998, 2013), (Shen 2005), Schamberg (1959a, 1959b), Nocilla (1962). The computation of aerodynamic coefficients of a space vehicle in high altitude flight, or in rarefied flows, is usually fulfilled by the Direct Simulation Monte Carlo (DSMC) method (Bird 1998, 2013), (Shen 2005). As Lord (1991), (Bird 1998, 2013) provided a DSMC implementation of the Cercignani-Lampis model, this model is known in literature as Cercignani-Lampis-Lord model and is labeled as CLL.

Each model provides different description of the molecule remission from the body surface and relies on different simplifying assumptions. All interaction models rely on the accommodation coefficients of energy or of the normal and tangential components of momentum. The accommodation coefficients are engineering parameters providing against the ignorance about the physical mechanism of the re-emission process. The values of all accommodation coefficients are between 0 and 1, defining the specular and the diffusive, fully accommodated re-emissions, respectively. The accommodation coefficients depend on a number of factors: gas composition, impact energy of the impinging molecules, temperature, material and roughness of the surface, angle of incidence.

Most of the DSMC computations are currently based on the assumption of diffusive, fully accommodated interaction. On the other hand, experiments verified that one can consider such a kind of interactions on engineering surface with contamination from air and with roughness of the surface. According to Bird (1998, 2013), this assumption should be reviewed whenever: i) a smooth surface has been exposed for long time to ultra-high vacuum, ii) a surface is heated, iii) the weight of the gas molecule is much smaller than the weight of the surface material, iv) the translational energy of the impinging molecules is larger than several electron-volts.

The present paper is the logical follow-on of a former article by Zuppardi *et al*. (2015) in which the effects of the Maxwell and the CLL models were compared by means of DSMC computations. In that paper, computer tests were carried out on three different cases: impact point on an elementary surface, aero-space-plane, a section of its wing. Both the Maxwell and CLL models ran with diffusive, fully accommodated, semi-specular (simulated by accommodation coefficients of 0.5) and specular accommodation coefficients, constant on the whole surface.

In the present paper the effects on the aerodynamic coefficients by the CLL and the Maxwell models, using the experimental, partial accommodation coefficients by Knetchel and Pitts (1973), are considered and compared with those by specular and diffusive, fully accommodated re-emission. Tests have been carried out on a NACA-0012 airfoil in clean and flapped configurations as function of the angle of attack, considering test conditions at an altitude of 100 km and a velocity of 7500 m/s. Like for the former, above mentioned paper (Zuppardi *et al*. 2015), due to the lack of experimental data at these conditions, a proper evaluation or validation of the models is not possible thus the aim of the present paper is just verifying and quantifying the differences of the results obtained with the two interaction models using the Knetchel and Pitts accommodation coefficients.

2. Accommodation coefficients

As said before, the gas-surface interaction includes incidence and re-emission of the molecules

upon and from the surface. The molecules, impinging upon the surface, are considered in equilibrium at temperature T_i and the molecules, re-emitted from the surface, are considered in equilibrium at temperature T_r; this can be different from the surface temperature T_w. An evaluation of the level at which T_r is adjusted toward T_w is provided by the energy (or thermal) accommodation coefficient (α_E)

$$\alpha_E = \frac{E_i - E_r}{E_i - E_w} \tag{1a}$$

where E is the molecule transitional energy, subscripts i, r and w are for incident, re-emitted and re-emitted at wall temperature. According to Bird (1998, 2013), the energy accommodation coefficients can be approximated by the fraction of molecules reflected diffusively. The accommodation coefficients are defined also in terms of the normal (α_n) and tangential (α_t) momentum components

$$\alpha_n = \frac{p_i - p_r}{p_i - p_w} \tag{1b}$$

$$\alpha_t = \frac{\tau_i - \tau_r}{\tau_i} \tag{1c}$$

where p is pressure and τ is shear stress. As summarized by Collins and Knox (1994), a number of measurements of momentum accommodation coefficients is reported in the open literature. These measurements involve different gases, surface materials and impact energies.

The Knetchel and Pitts (1973) measurements of the momentum partial accommodation coefficients are interesting for the present application because obtained at conditions pretty close to Earth re-entry. Knetchel and Pitts carried out measurements in the interval of E_i between 10 and 40 eV, considering as specimen an elementary surface of aluminum and as gas nitrogen. They evaluated the following least square curves fitting the results in the range of the angle of incidence $0 \leq \vartheta \leq 90$ deg

$$\alpha_n = 1.00 - 0.9 \exp(-0.280 E_i \cos^2 \varphi) \tag{2a}$$

$$\alpha_t = 0.90 - 1.20 \exp(-0.147 E_i \sin^{3/4} \varphi) \tag{2b}$$

where φ is complementary to the incidence angle ϑ ($\varphi = \pi/2 - \vartheta$). In the present application, ϑ includes the geometrical incidence angle ϑ_g ($\vartheta_g = \tan^{-1}(dy/dx)$, $y = y(x)$ defines the airfoil surface) and the angle of attack AoA

$$\vartheta = \vartheta_g \pm \text{AoA} \tag{3}$$

plus and minus symbols are for the points on the lower and the upper surface, respectively.

3. Maxwell and Cercignani-Lampis-Lord models

The DSMC implementation of the Maxwell and the Cercignani-Lampis-Lord models starts

with the computation of the velocity components (u_i, v_i, w_i) of each molecule impinging upon the surface. This velocity is composed of the free stream velocity $\underline{V}_\infty$ ($V_{\infty x}$, $V_{\infty y}$, $V_{\infty z}$) and the molecular thermal velocity $\underline{C}_i$ (U_i, V_i, W_i) (Bird 1998, 2013)

$$u_i = V_{\infty x} + U_i \tag{4.a}$$

$$v_i = V_{\infty y} + V_i \tag{4.b}$$

$$w_i = V_{\infty z} + W_i \tag{4.c}$$

where u_i is the normal component and v_i and w_i are the tangent components of velocity to the surface (Bird 1998, 2013). The components of $\underline{C}_i$ are set in turn at random from the most probable molecular velocity (c) at temperature T_∞

$$c(T_\infty) = \sqrt{2\frac{k}{m}T_\infty} \tag{5}$$

where k is the Boltzmann constant and m is the mass of a molecule

$$U_i, V_i, W_i = \sin(2\pi R)c(T_\infty)\sqrt{-\ln R} \tag{6}$$

where R is a random number ($0 \le R \le 1$), different in each formula:

According to Maxwell, the reflection is governed by the "classical" specular and diffusive models. The specular model assumes that the normal component of the reflected velocity is reversed: $u_r = -u_i$, and the tangential components do not change: $v_r = v_i$, $w_r = w_i$. In the DSMC implementation, the diffusive model is considered always fully accommodated at the surface temperature. This implies that the components of the velocity of the molecules, re-emitted diffusively, are computed at random from the most probable molecular velocity in equilibrium at the wall temperature, ($c(T_w)$, Eq. (5))

$$U_r = c(T_w)\sqrt{-\ln R} \tag{7.a}$$

$$V_r = c(T_w)\sqrt{-\ln R} * \sin(2\pi R) \tag{7.b}$$

$$W_r = c(T_w)\sqrt{-\ln R} * \cos(2\pi R) \tag{7.c}$$

The normal and tangential components of the stress are linked to the incident and reflected momentum; the resultant pressure and shear stress read

$$p = (1+f)p_i + (1-f)p_w \tag{8.a}$$

$$\tau = (1-f)\tau_i \tag{8.b}$$

where f is the fraction of molecules re-emitted specularly.

The Cercignani-Lampis model provides the probabilities that an incident molecule with normal velocity component U_i is reflected with normal velocity component U_r and the tangential component V_i (or W_i) is reflected with tangential velocity V_r (or W_r)

$$P(U_r, U_i) = \left(\frac{2U_r}{\alpha_{En}}\right)I_0\left\{\frac{2(1-\alpha_{En})^{1/2}U_iU_r}{\alpha_{En}}\right\}\exp\left\{\frac{U_r^2 + (1-\alpha_{En})U_i^2}{\alpha_{En}}\right\} \tag{9a}$$

$$P(V_r, V_i) = (\pi \alpha_t)^{-1/2} \exp\left[-\frac{\left\{ V_r - (1-\alpha_t)^{1/2} V_i \right\}^2}{\alpha_t} \right] \tag{9b}$$

where the components of velocity are made non-dimensional by the most probable molecular speed at the wall temperature, I_0 is the Bessel function of zero[th] order and α_{En} is the kinetic energy accommodation coefficient associated with the normal component of velocity. Eq. (9b) holds also for $P(W_r, W_i)$. Considering that the energy accommodation coefficient is related only to the kinetic energy, in the present computations, α_{En} is approximated by α_n: $\alpha_{En} \cong \alpha_n$.

The DSMC implementation by Lord consists in the following equations computing the components of the reflected velocity

$$U_r = (r^2 + (1-\alpha)U_i^2 + 2r(1-\alpha)^{1/2}U_i \cos\theta)^{1/2} \tag{10a}$$

$$V_r = (1-\alpha)^{1/2}V_i + r\cos\theta \tag{10b}$$

$$W_r = r\sin\theta \tag{10c}$$

where θ and r are random quantities

$$\theta = 2\pi R \tag{10d}$$

$$r = \sqrt{-\alpha \ln(R)} \tag{10e}$$

and $\alpha = \alpha_n$ for the normal component (U_r), $\alpha = \alpha_t(2-\alpha_t)$ for the tangential components (V_r and W_r). The CLL model reduces to the specular and to the diffusive model when both α_n and α_t are zero or unity, respectively.

The resultant pressure and shear stress read

$$p = p_i + p_r \tag{11a}$$

$$\tau = \tau_i - \tau_r \tag{11b}$$

4. Direct simulation Monte Carlo code

It is well known that the DSMC method (Bird 1998, 2013, Shen 2005) is currently the only tool for the solution of rarefied flow fields from continuum low density to free molecular regimes. In fact, the Navier-Stokes equations fail in low density regimes. The failure is due to the failure of the "classical" laws by Newton, Fourier and Fick, computing the transport parameters.

DSMC considers the gas as made up of molecules. It is based on the kinetic theory of gas and computes the evolution of millions of simulated molecules, each one representing a large number (say 10^{15}) of real molecules in the physical space. The molecule-molecule and molecule-surface collisions are taken into account. The computational domain is divided in cells. The cells are used for selecting the colliding molecules and for sampling the macroscopic fluid-dynamic quantities.

The most important advantage is that the method does not suffer from numerical instabilities and does not rely on similarity parameters, like the Mach and the Reynolds numbers. On the other hand, the method is inherently unsteady; a steady solution is achieved after a sufficiently long simulation time.

The computation of the distributions of pressure and shear stress along the body surface and then of the global aerodynamic coefficients was carried by the DS2V-64 bits code (Bird 2005). DS2V considers air as made up of five neutral reacting species (O_2, N_2, O, N and NO) and rely on the built-in Gupta-Yos-Thompson (1989) chemical model, consisting of 23 reactions. The code implements both the Maxwell and the CLL models. The diffusive, fully accommodated Maxwell model is the default option. The user can change the gas-surface interaction by inputting the fraction (f) of molecules re-emitted specularly.

DS2V is "sophisticated". As widely reported in literature (Bird 2004, 2006, 2009, Gallis 2009), this code implements computing procedures providing efficiency and accuracy higher than those from a "basic" DSMC code. Besides being "sophisticated", DS2V is also "advanced", allowing the user to evaluate the quality of a simulation. The user can verify, by the on line visualization of the ratio between the molecule mean collision separation (mcs) and the mean free path (λ) in each computational cell, that the number of simulated molecules and collision cells are adequate. In addition, the code allows the user to change (or to increase), during a run, the number of simulated molecules.

The ratio mcs/λ has to be less than unity everywhere in the computational domain. Bird (2005) suggests 0.2 as a limit value for an optimal quality of the run. In addition, the code gives the user information about the stabilization of the runs by means of the profile of the number of simulated molecules as a function of the simulated time. The stabilization of a DS2V calculation is achieved when this profile becomes jagged and included within a band defined by the standard deviation of the number of simulated molecules.

5. Test conditions

The chord (*c*) of the tested NACA-0012 airfoil is 2 m and the position of the flap hinge is at 1.30 m from the leading edge or at 65% of the chord. Simulations were carried out varying the angle of attack (AoA) in the range 0-50 deg with a spacing of 5 deg and considering the flap deflections: δ=0, 20, 40 deg. The airfoil surface was approximated by 50 linear panels on the upper and on the lower surfaces. The computational region was a rectangle: L_x=2.4 m, L_y=1.2 m.

The free stream conditions, provided by the US standard Atmosphere 1976, are reported in

Table 1(a) Free stream test conditions

Altitude (*h*)	100 km
Temperature (T_∞)	196 K
Density (ρ_∞),	5.59×10^{-7} Kg/m^3
Number density (N_∞)	1.19×10^{19} m^{-3}
Mean free path (λ_∞)	0.14 m
Molar fraction of Oxygen (α_{O2})	0.17978
Molar fraction of Nitrogen (α_{N2})	0.77504
Molar fraction of atomic Oxygen (α_O)	0.04518

Table 1(b) Flight conditions and aerodynamic parameters

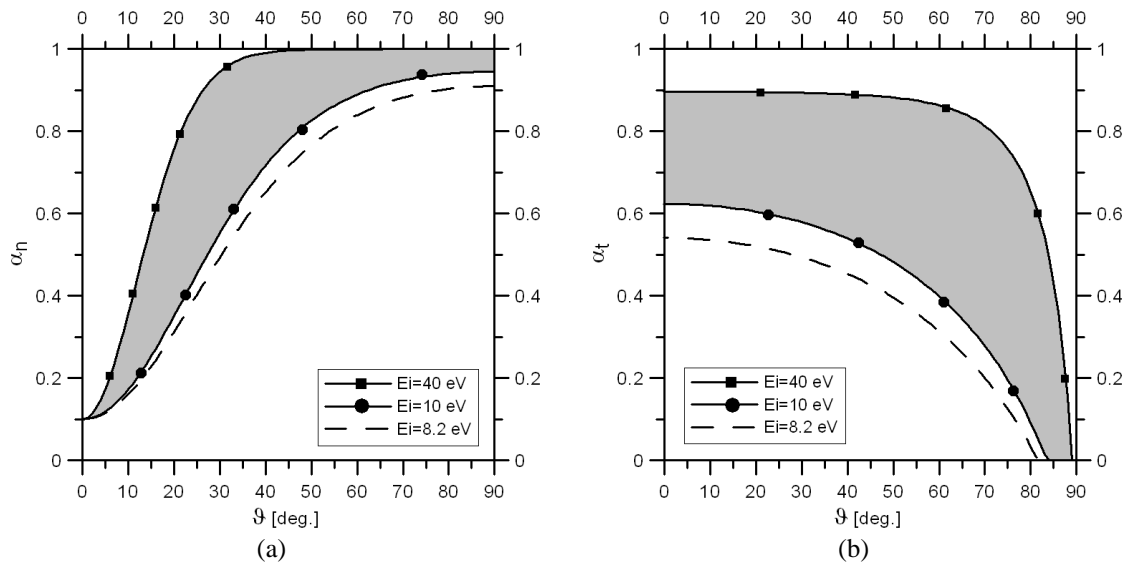|	
Velocity (V_∞)	7500 m/s
Wall temperature (T_w)	300 K
Mach number (M_∞)	26
Reynolds number ($Re_{\infty c}$)	632
Knudsen number ($Kn_{\infty c}$)	0.06

Fig. 1 Normal (a) and tangential (b) momentum accommodation coefficients as functions of the local angle of incidence and impact energy

Table 1(a). The flight conditions or the Mach, Reynolds and Knudsen numbers, based on the airfoil chord, are reported in Table 1(b). The wall was considered non-catalytic and temperature (T_w) was constant along the whole body. The Knudsen number indicates that the flow field is in continuum low density regime. In fact, according to Moss (1995), the transitional regime is defined by: $10^{-3} < Kn_{\infty c} < 50$.

Figs. 1(a), 1(b) show the profiles of α_n and α_t as functions of ϑ and impact energy (E_i). According to the Knetchel and Pitts measurements, the proper values of α_n and α_t are identified by the grey area, included between the curves, computed by Eqs. (2a) and (2b) with E_i=40 eV and E_i=10 eV, respectively. The dashed curve was computed with the impact energy of 8.2 eV, corresponding to the test velocity and considering the mass of a molecule of 4.68×10^{-26} kg; this mass was evaluated as an average of the air components weighted on the molar fraction. Figs. 1(a) and 1(b) verify that the values of α_n and α_t, with E_i=8.2 compare reasonably well with those obtained with E_i=10 eV.

Figs. 2(a) to 2(d) show the profiles of the Knetchel and Pitts normal and tangential accommodation coefficients on the upper (a, b) and lower (c, d) surfaces of the airfoil at the intermediate angle of attack of 25 deg and with the three flap deflections. The discontinuity in the profiles of the curves at the flap hinge position is due to the abrupt change of ϑ. As expected, the higher the flap deflection the higher α_n and the lower α_t.
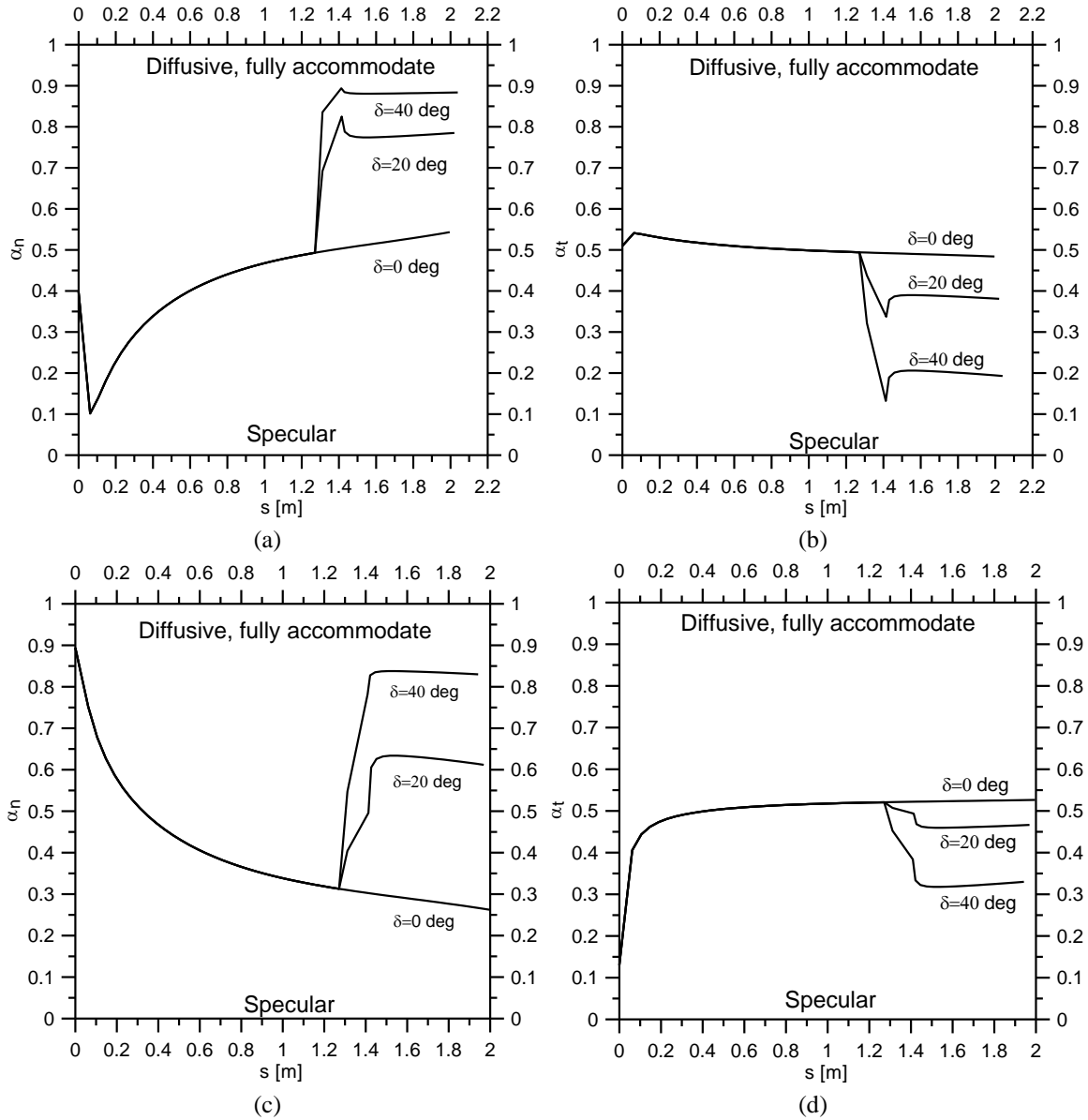
Fig. 2 Normal and tangential momentum accommodation coefficients along the airfoil upper (a, b) and lower (c, d) surfaces with the three flap deflection: AoA=25 deg

In the present paper, the Knetchel and Pitts coefficients are used also to evaluate the effect of the incidence angle on the fraction of molecules re-emitted specularly, therefore on the Maxwell model implemented in DS2V (Eqs. (8a), (8b)). The related results will be defined as "partially specular". The fraction "*f*", along the airfoil surface, reads

$$f = 1 - \sqrt{\alpha_n^2 + \alpha_t^2} \tag{13}$$
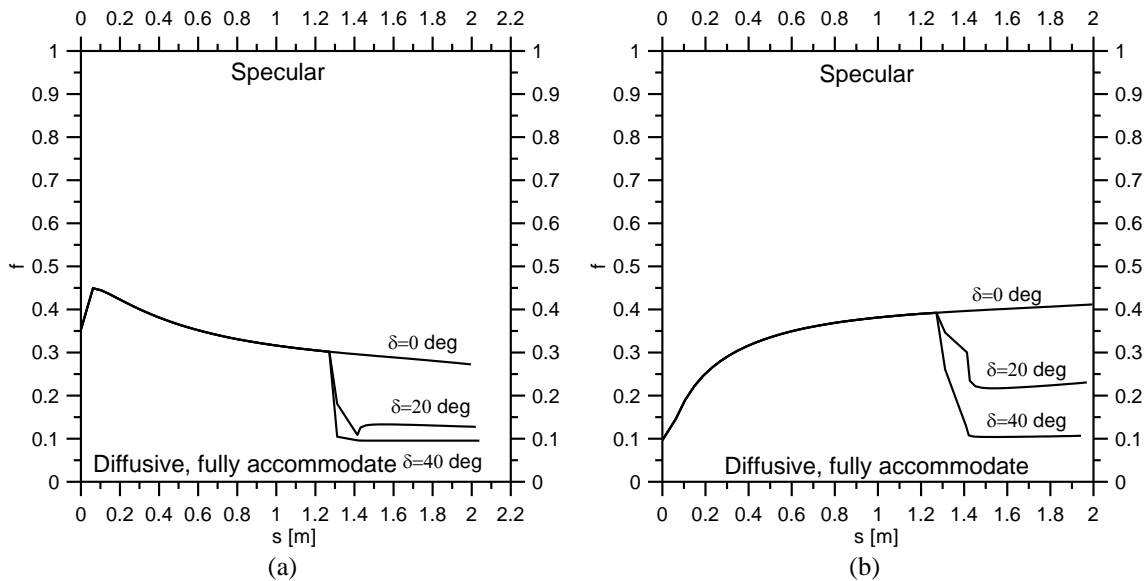
Fig. 3 Fraction of molecules re-emitted specularly along the airfoil upper (a) and lower (b) surface with the three flap deflection: AoA=25 deg

Figs. 3(a) and 3(b) show the profiles of "*f*" along the upper (a) and lower (b) surfaces.

6. Accuracy of the computations

The DS2V code generates automatically the computational grid on the basis of the input number of available megabytes of the computer and of the free stream molecule number density. The input number of megabytes has been 1200 for all tests. The user can only roughly control the number of cells by setting the input number of divisions and elements in each division; the higher the number of elements the higher the number of the cells after the adaptation process. DS2V suggests an optimal number of molecules/cell for adapting both collision and sampling cells. An increment of the number of cells can be achieved also by inputting a smaller number of molecules/cell. A sensitivity analysis of the results in terms of number of cells was already successfully carried out by Zuppardi *et al.* (2015) considering the global aerodynamic coefficients of a wing section of the aero-space-plane SpaceLiner.

The present analysis relies on 132 runs or 11 angles of attack, 3 flap deflections and 4 re-emission models: Maxell Diffusive, Fully Accommodated, Maxwell SPEcular, Maxwell Partially SPecular, Cercignani-Lampis-Lord; the related results will be labeled on the tables as DFA, SPE, PSP and CLL, respectively. As no experimental data are available in open literature at the present test conditions, the accuracy of the computations is provided only by a correct use of the code in terms of both fluid-dynamic and DSMC simulations. All runs satisfied the requirement for a correct fluid-dynamic simulation in terms of simulation time (t_s) and quantified by the ratio t_s/t_f where t_f is the time to travel the airfoil chord at the free stream velocity. A rule of the thumb suggests considering a run stabilized from a fluid-dynamic point of view when $t_s/t_f \cong 10$ and, as said before, a correct DSMC simulation is achieved when mcs/$\lambda \leq 0.2$. For example, Tables 2 reports

Table 2 Run parameters at AoA=50 deg and δ=40 deg

	DFA	SPE	PSP	CLL
mcs/λ	4.2×10^{-2}	4.2×10^{-3}	3.3×10^{-2}	3.3×10^{-2}
t_s/t_f	6.4	7.4	7.2	7.4

these parameters for the four interaction models at the most severe conditions for a DSMC computation, i.e., AoA=50 deg and δ=40 deg.

7. Analysis of the results

Figs. 4(a) to 4(d) show the profiles of the lift C_l (a), drag C_d (b), longitudinal moment C_m (c) (the reduction pole is the airfoil leading edge) coefficients and of the aerodynamic efficiency E ($E=C_l/C_d$) (d) as functions of the angle of attack at the intermediate flap deflection (δ=20 deg). Figures show that the coefficients, computed by the CLL and the Maxwell "partially specular" gas-surface interaction models are pretty close to those computed by the Maxwell diffusive, fully accommodated interaction model. This trend increases with the angle of attack; in fact the higher the angle of attack the higher the angle of incidence and therefore, by Eqs. (2a) and (2b), the higher α_n and the lower α_t. A relevant difference has been found for C_l and particularly for C_d, (therefore amplified in E), with those computed by the specular interaction model. In fact, as the specular model does not provide tangential stress, drag is under-estimated. The same remark holds also for the results obtained with δ=0 and δ=40 deg.

(a)

(b)
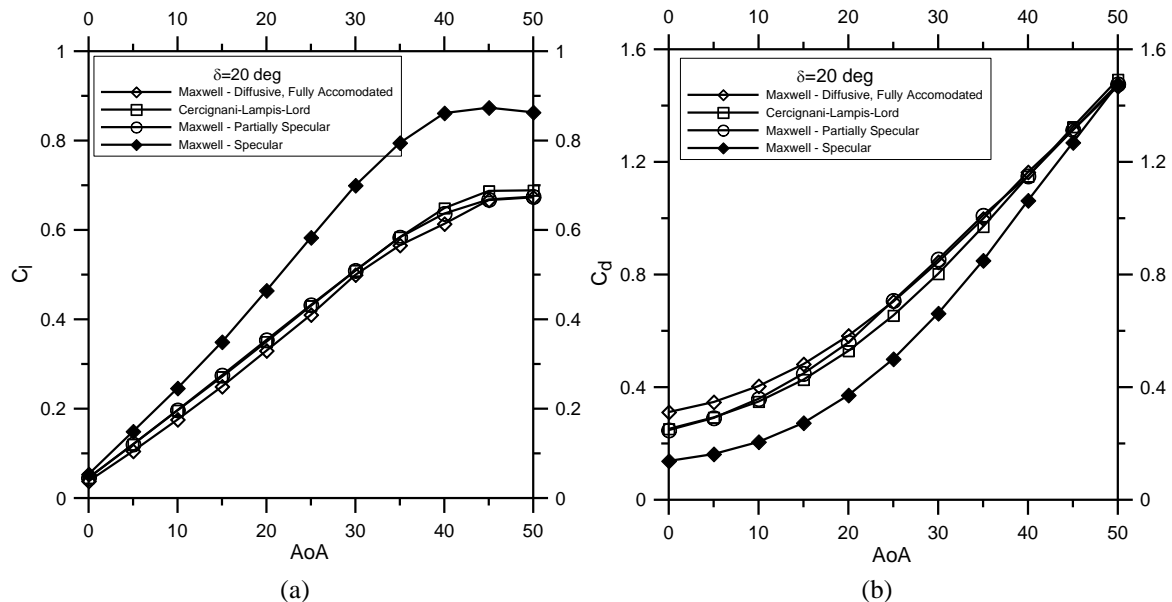
Fig. 4 Profiles of the lift (a), drag (b), longitudinal moment (c) coefficients and aerodynamic efficiency (d) of the airfoil with δ=20 deg by the Maxwell and CLL models

(c)   (d)
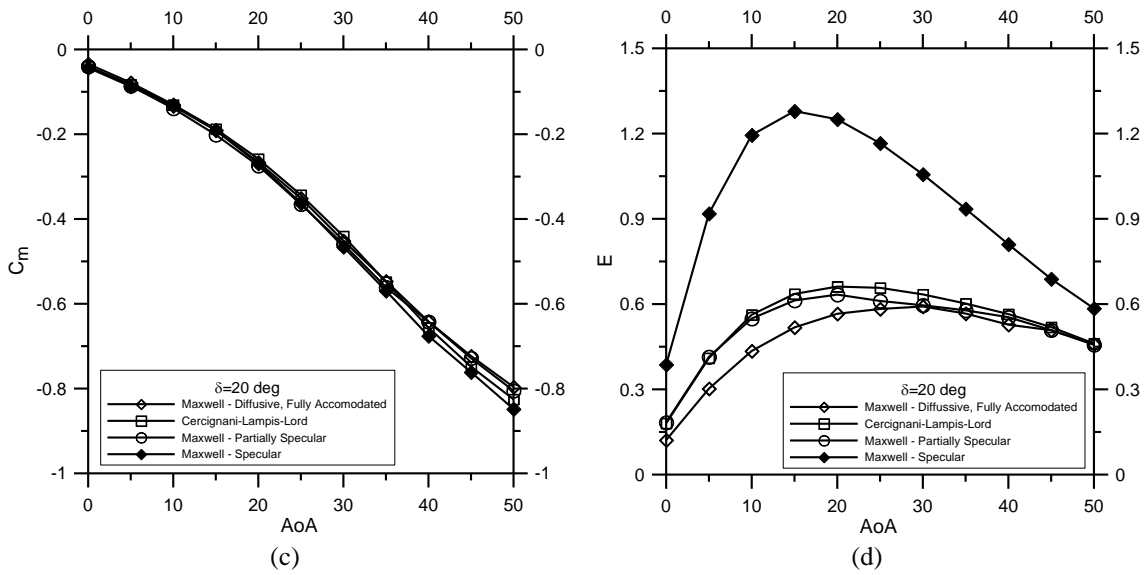
Fig. 4 Continued

Figs. 5(a) to 5(e) show the profiles of the local aerodynamic coefficients of pressure C_p (a), skin friction C_f (b), heat flux C_h (c) and, for completeness, of slip velocity V_s (d) and slip temperature T_s (e) along the airfoil lower surface as functions of the curvilinear abscissa (s) at the intermediate flap deflection and intermediate angle of attack (δ=20 deg, AoA=25 deg). Figs. 5(a) and 5(c) show that the interaction model does not influence strongly the coefficients of pressure and of heat flux, even on the flap surface. On the contrary, a relevant difference has to be pointed out for the skin

(a)   (b)
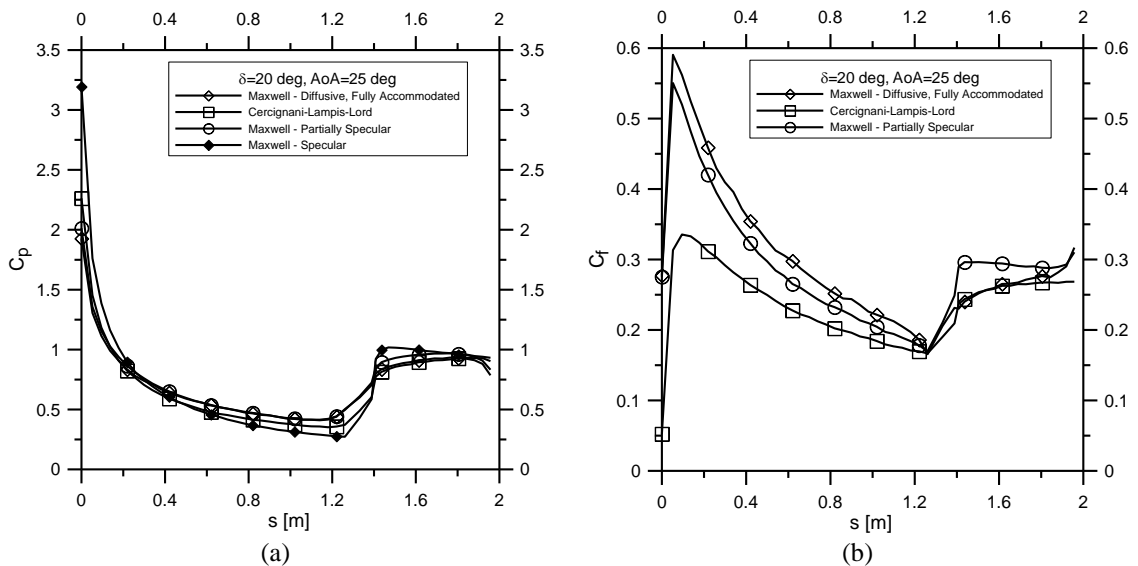
Fig. 5 Profiles of the pressure (a), skin friction (b), heat flux (c) coefficients and of slip velocity (d) and slip temperature (e) by the Maxwell and CLL models along the airfoil lower surface: AoA=25 deg, δ=20 deg

(c)

(d)

(e)
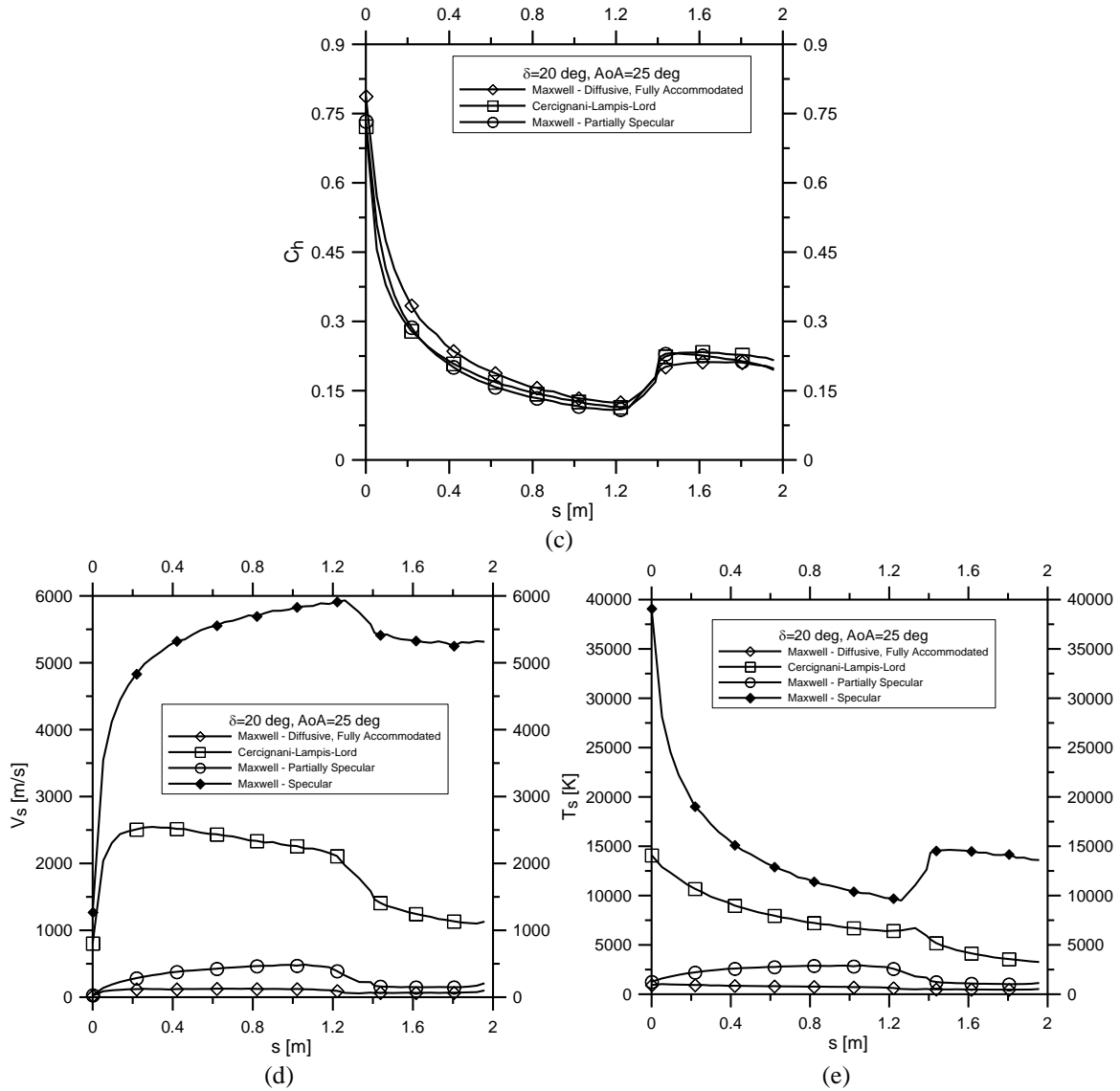
Fig. 5 Continued

friction coefficient computed by the CLL model (Fig. 5(b)). This is probably due to the fact that, in the CLL model, α_t and α_n work independently while in the Maxwell "partially specular" model, the two accommodation coefficients contribute together in the evaluation of the fraction of molecules specularly re-emitted (see Eq. (13)). As expected, Figs. 5(d) and 5(e) verify that the gas-surface interaction model influences mostly the slip velocity and the slip temperature.

As most of the DSMC computations are currently based on the assumption of diffusive, fully accommodated interaction, the effects of the interaction model are quantified by the ratios of the global and the local aerodynamic coefficients with those computed by the Maxwell diffusive, fully accommodated model. For all angles of attack, Tables 3, 4 and 5 report the ratios for the global

Table 3 Ratios of global airfoil aerodynamic coefficients between the CLL and Maxwell models: δ=0 deg

AoA [deg]	$\frac{C_{lSPE}}{C_{lDFA}}$	$\frac{C_{lCLL}}{C_{lDFA}}$	$\frac{C_{lPSP}}{C_{lDFA}}$	$\frac{C_{dSPE}}{C_{dDFA}}$	$\frac{C_{dCLL}}{C_{dDFA}}$	$\frac{C_{dPSP}}{C_{dDFA}}$	$\frac{E_{SPE}}{E_{DFA}}$	$\frac{E_{CLL}}{E_{DFA}}$	$\frac{E_{PSP}}{E_{DFA}}$	$\frac{C_{mSPE}}{C_{mDFA}}$	$\frac{C_{mCLL}}{C_{mDFA}}$	$\frac{C_{mPSP}}{C_{mDFA}}$
0	--	--	--	0.44	0.74	0.75	--	--	--	0.25	0.63	0.71
5	0.93	1.01	1.03	0.44	0.76	0.77	2.10	1.34	1.33	0.30	0.74	0.86
10	1.04	0.97	0.98	0.45	0.78	0.80	2.29	1.25	1.23	0.43	0.73	0.83
15	1.12	0.98	1.01	0.48	0.81	0.85	2.32	1.21	1.18	0.53	0.79	0.89
20	1.18	1.02	1.02	0.53	0.85	0.91	2.25	1.21	1.11	0.62	0.86	0.95
25	1.24	1.03	1.04	0.58	0.88	0.95	2.14	1.17	1.09	0.71	0.91	1.00
30	1.30	1.04	1.05	0.64	0.92	0.99	2.02	1.13	1.08	0.79	0.96	1.04
35	1.35	1.03	1.04	0.73	0.94	0.99	1.85	1.09	1.05	0.86	0.98	1.02
40	1.37	1.06	1.05	0.80	0.99	1.00	1.70	1.07	1.05	0.91	1.03	1.04
45	1.35	1.05	1.04	0.87	0.99	1.01	1.54	1.06	1.03	0.95	1.02	1.04
50	1.33	1.06	1.05	0.93	1.00	1.04	1.44	1.06	1.01	0.98	1.03	1.07

Table 4 Ratios of global airfoil aerodynamic coefficients between the CLL and Maxwell models: δ=20 deg

AoA [deg]	$\frac{C_{lSPE}}{C_{lDFA}}$	$\frac{C_{lCLL}}{C_{lDFA}}$	$\frac{C_{lPSP}}{C_{lDFA}}$	$\frac{C_{dSPE}}{C_{dDFA}}$	$\frac{C_{dCLL}}{C_{dDFA}}$	$\frac{C_{dPSP}}{C_{dDFA}}$	$\frac{E_{SPE}}{E_{DFA}}$	$\frac{E_{CLL}}{E_{DFA}}$	$\frac{E_{PSP}}{E_{DFA}}$	$\frac{C_{mSPE}}{C_{mDFA}}$	$\frac{C_{mCLL}}{C_{mDFA}}$	$\frac{C_{mPSP}}{C_{mDFA}}$
0	1.41	1.20	1.20	0.44	0.81	0.79	3.19	1.49	1.51	1.27	1.18	1.17
5	1.42	1.43	1.15	0.47	0.84	0.84	3.04	1.36	1.37	1.11	1.05	1.10
10	1.40	1.12	1.12	0.51	0.86	0.89	2.75	1.29	1.26	1.03	1.00	1.07
15	1.40	1.07	1.10	0.57	0.89	0.93	2.47	1.23	1.18	1.00	0.99	1.06
20	1.41	1.06	1.07	0.64	0.91	0.96	2.21	1.17	1.12	1.01	0.97	1.03
25	1.42	1.05	1.05	0.71	0.93	1.01	2.00	1.13	1.05	1.03	0.98	1.04
30	1.40	1.02	1.02	0.78	0.95	1.01	1.79	1.07	1.01	1.03	0.98	1.02
35	1.41	1.03	1.03	0.85	0.97	1.01	1.65	1.06	1.02	1.04	1.00	1.03
40	1.40	1.06	1.04	0.91	0.99	0.99	1.54	1.07	1.05	1.05	1.02	1.00
45	1.31	1.03	1.00	0.97	1.01	1.00	1.36	1.02	1.00	1.05	1.03	1.01
50	1.28	1.02	1.00	1.01	1.02	1.01	1.28	1.01	1.00	1.07	1.04	1.01

aerodynamic coefficients and Tables 6, 7 and 8 report the ratios for the local coefficients and slip velocity for the three flap deflections. For the local coefficients and slip velocity, the ratios are computed considering, as representative value, the average on the airfoil lower surface. The ratios, involving the slip temperature, are comparable with those involving the slip velocity and are not reported here for the sake of shortness.

The present ratios confirm the equivalence of the Maxwell and the CLL models, already found by Zuppardi *et al*. (2015) where fully accommodated coefficients ($\alpha_n=\alpha_t=1$, $f=0$) were considered along the airfoil surface. In fact, all ratios, including both the global and the local coefficients, are pretty close to 1. The ratios, computed by the CLL and the Maxwell "partially specular" models, tend to unity with increasing the angle of attack because, as already shown in Fig. 1, both models rely on the Knetchel and Pitts accommodation coefficients that tend to the diffusive re-emission by increasing the angle of incidence.

Table 5 Ratios of global airfoil aerodynamic coefficients between the CLL and Maxwell models: δ=40 deg

AoA [deg]	$\dfrac{C_{lSPE}}{C_{lDFA}}$	$\dfrac{C_{lCLL}}{C_{lDFA}}$	$\dfrac{C_{lPSP}}{C_{lDFA}}$	$\dfrac{C_{dSPE}}{C_{dDFA}}$	$\dfrac{C_{dCLL}}{C_{dDFA}}$	$\dfrac{C_{dPSP}}{C_{dDFA}}$	$\dfrac{E_{SPE}}{E_{DFA}}$	$\dfrac{E_{CLL}}{E_{DFA}}$	$\dfrac{E_{PSP}}{E_{DFA}}$	$\dfrac{C_{mSPE}}{C_{mDFA}}$	$\dfrac{C_{mCLL}}{C_{mDFA}}$	$\dfrac{C_{mPSP}}{C_{mDFA}}$
0	2.21	1.29	1.20	0.69	0.93	0.93	3.20	1.39	1.30	1.97	1.27	1.20
5	1.90	1.14	1.11	0.79	0.93	0.95	2.42	1.23	1.17	1.67	1.09	1.10
10	1.63	1.05	1.06	0.82	0.93	0.97	1.98	1.13	1.09	1.38	1.00	1.04
15	1.49	1.01	1.03	0.86	0.94	0.99	1.73	1.08	1.04	1.25	0.97	1.02
20	1.43	1.02	1.02	0.92	0.97	0.99	1.56	1.05	1.04	1.21	1.00	1.01
25	1.33	1.00	1.01	0.93	0.98	0.98	1.45	1.03	1.04	1.13	1.00	1.00
30	1.31	1.03	1.01	0.96	0.99	0.98	1.36	1.04	1.03	1.10	1.01	0.99
35	1.34	1.03	1.02	1.00	1.00	0.99	1.34	1.03	1.03	1.12	1.03	0.99
40	1.31	1.03	1.00	1.01	1.00	0.99	1.30	1.03	1.01	1.09	1.03	0.99
45	1.29	1.04	1.02	1.03	1.00	0.99	1.25	1.04	1.04	1.08	1.03	0.99
50	1.24	1.05	1.02	1.04	1.00	0.99	1.20	1.04	1.03	1.06	1.03	0.99

Table 6 Ratios of local airfoil aerodynamic coefficients between the CLL and Maxwell models: δ=0 deg

AoA [deg]	$\dfrac{C_{pSPE}}{C_{pDIF}}$	$\dfrac{C_{pCLL}}{C_{pDIF}}$	$\dfrac{C_{pPSP}}{C_{pDIF}}$	$\dfrac{C_{fSPE}}{C_{fDIF}}$	$\dfrac{C_{fCLL}}{C_{fDIF}}$	$\dfrac{C_{fPSP}}{C_{fDIF}}$	$\dfrac{C_{hSPE}}{C_{hDIF}}$	$\dfrac{C_{hCLL}}{C_{hDIF}}$	$\dfrac{C_{hfPSP}}{C_{hDIF}}$	$\dfrac{V_{sSPE}}{V_{sDIF}}$	$\dfrac{V_{sCLL}}{V_{sDIF}}$	$\dfrac{V_{sPSP}}{V_{sDIF}}$
0	0.79	0.82	0.90	0.00	0.56	0.63	0.00	0.75	0.65	19.71	11.23	4.25
5	0.79	0.86	0.93	0.00	0.63	0.68	0.00	0.82	0.69	22.90	13.73	4.48
10	0.84	0.87	0.92	0.00	0.66	0.72	0.00	0.84	0.71	31.84	16.09	4.83
15	0.89	0.90	0.95	0.00	0.70	0.79	0.00	0.86	0.76	36.49	17.65	4.59
20	0.92	0.94	0.98	0.00	0.72	0.87	0.00	0.87	0.82	41.15	18.32	4.27
25	0.95	0.95	1.01	0.00	0.75	0.91	0.00	0.89	0.86	46.92	19.09	3.79
30	0.98	0.97	1.02	0.00	0.81	0.96	0.00	0.94	0.90	51.63	19.70	3.20
35	1.02	0.98	1.02	0.00	0.86	0.95	0.00	0.97	0.91	58.83	19.84	3.89
40	1.04	1.01	1.03	0.00	0.90	0.96	0.00	1.02	0.93	59.87	18.53	2.18
45	1.04	1.01	1.02	0.00	0.86	0.99	0.00	1.01	0.96	62.10	16.48	1.86
50	1.06	1.02	1.05	0.00	0.84	1.05	0.00	1.02	1.00	65.02	15.68	1.72

Table 7 Ratios of local airfoil aerodynamic coefficients between the CLL and Maxwell models: δ=20 deg

AoA [deg]	$\dfrac{C_{pSPE}}{C_{pDIF}}$	$\dfrac{C_{pCLL}}{C_{pDIF}}$	$\dfrac{C_{pPSP}}{C_{pDIF}}$	$\dfrac{C_{fSPE}}{C_{fDIF}}$	$\dfrac{C_{fCLL}}{C_{fDIF}}$	$\dfrac{C_{fPSP}}{C_{fDIF}}$	$\dfrac{C_{hSPE}}{C_{hDIF}}$	$\dfrac{C_{hCLL}}{C_{hDIF}}$	$\dfrac{C_{hfPSP}}{C_{hDIF}}$	$\dfrac{V_{sSPE}}{V_{sDIF}}$	$\dfrac{V_{sCLL}}{V_{sDIF}}$	$\dfrac{V_{sPSP}}{V_{sDIF}}$
0	0.94	0.94	0.98	0.00	0.71	0.71	0.00	0.90	0.70	26.86	14.67	4.38
5	1.00	0.97	1.01	0.00	0.76	0.78	0.00	0.93	0.76	32.62	16.76	4.45
10	1.01	0.98	1.03	0.00	0.76	0.83	0.00	0.92	0.80	37.83	20.17	4.22
15	1.03	0.98	1.04	0.00	0.77	0.86	0.00	0.92	0.83	43.43	19.07	3.93
20	1.04	0.98	1.03	0.00	0.78	0.90	0.00	0.93	0.86	48.35	19.54	3.49
25	1.05	0.98	1.03	0.00	0.81	0.98	0.00	0.95	0.93	54.36	19.82	3.22
30	1.05	0.97	1.02	0.00	0.85	1.01	0.00	0.98	0.96	63.04	20.35	2.69
35	1.06	0.99	1.02	0.00	0.86	1.00	0.00	1.00	0.96	68.43	19.60	2.23
40	1.07	1.01	1.01	0.00	0.84	0.92	0.00	0.99	0.92	70.22	18.02	1.79
45	1.06	1.02	1.00	0.00	0.88	1.00	0.00	1.04	0.97	74.11	18.23	1.67
50	1.07	1.02	1.07	0.00	0.89	1.01	0.00	1.06	0.98	74.52	18.48	1.57

Table 8 Ratios of local airfoil aerodynamic coefficients between the CLL and Maxwell models: δ=40 deg

AoA [deg]	$\dfrac{C_{pSPE}}{C_{pDIF}}$	$\dfrac{C_{pCLL}}{C_{pDIF}}$	$\dfrac{C_{pPSP}}{C_{pDIF}}$	$\dfrac{C_{fSPE}}{C_{fDIF}}$	$\dfrac{C_{fCLL}}{C_{fDIF}}$	$\dfrac{C_{fPSP}}{C_{fDIF}}$	$\dfrac{C_{hSPE}}{C_{hDIF}}$	$\dfrac{C_{hCLL}}{C_{hDIF}}$	$\dfrac{C_{hfPSP}}{C_{hDIF}}$	$\dfrac{V_{sSPE}}{V_{sDIF}}$	$\dfrac{V_{sCLL}}{V_{sDIF}}$	$\dfrac{V_{sPSP}}{V_{sDIF}}$
0	1.42	1.12	1.11	0.00	0.81	0.88	0.00	0.98	0.87	31.12	16.22	4.11
5	1.35	1.04	1.07	0.00	0.80	0.91	0.00	0.97	0.90	38.08	17.92	4.15
10	1.23	0.99	1.04	0.00	0.81	0.92	0.00	0.98	0.91	44.01	19.01	4.04
15	1.17	0.98	1.02	0.00	0.83	0.95	0.00	0.99	0.93	50.23	20.18	3.83
20	1.16	1.00	1.02	0.00	0.83	0.94	0.00	1.01	0.93	56.53	20.91	3.47
25	1.11	1.00	1.00	0.00	0.83	0.94	0.00	1.01	0.93	62.99	21.53	3.02
30	1.09	1.01	1.00	0.00	0.82	0.95	0.00	1.00	0.94	67.52	21.55	2.55
35	1.11	1.01	1.00	0.00	0.83	0.95	0.00	1.01	0.94	71.72	22.26	2.13
40	1.09	1.01	1.00	0.00	0.82	0.97	0.00	1.02	0.96	70.92	22.86	1.83
45	1.09	1.01	1.00	0.00	0.74	0.92	0.00	1.02	0.94	67.96	24.32	1.50
50	1.07	1.01	1.00	0.00	0.65	0.92	0.00	1.03	0.95	60.30	27.30	1.40

8. Conclusions

The Maxwell and the Cercignani-Lampis-Lord gas-surface interaction models have been compared in hypersonic, rarefied flow, considering both global and local aerodynamic coefficients of a NACA-0012 airfoil in clean and flapped configurations. Computer tests have been carried out by the DSMC code DS2V-64 bits in the range of angles of attack 0-50 deg and flap deflection of 0, 20 and 40 deg.

The Cercignani-Lampis-Lord model has been tested using the Knetchel and Pitts partial, normal and tangential momentum accommodation coefficients. The Maxwell model has been tested considering, besides the "classical" specular and diffusive, fully accommodated models, also a "partially specular" model, obtained by combining the Knetchel and Pitts accommodation coefficients. The results confirmed what already found in a former paper by the present author that the Maxwell and the Cercignani-Lampis-Lord models are practically equivalent. On the opposite, the differences of the Maxwell diffusive fully accommodated model with the specular one are relevant.

The present results are interesting from both a scientific and an operational point of view. The scientific interest derives from the experimental nature of the Knetchel and Pitts accommodation coefficients. The use of the Maxwell diffusive fully accommodated model implies simple and immediate computations, making the model the most appropriate for DSMC codes in space applications.

References

Bird, G.A. (1998), *Molecular Gas Dynamics and Direct Simulation Monte Carlo*, Clarendon Press, Oxford, Great Britain.

Bird, G.A. (2004), "The DS2V/3V program suite for DSMC calculations", *Proceedings of the 24th International Symposium on Rarafied Gas Dynamics*, edited by M. Capitelli, Monopoli, Italy, July.

Bird, G.A. (2005), *The DS2V Program User's Guide Ver. 3.2*, G.A.B. Consulting Pty Ltd, Sydney,

Australia.

Bird, G.A. (2006), "Sophisticated versus simple DSMC", *Proceedings of the 25th International Symposium on Rarefied Gas Dynamics*, Saint Petersburg, Russia, July.

Bird, G.A., Gallis, M.A., Torczynski, J.R. and Rader, D.J. (2009), "Accuracy and efficiency of the sophisticated direct simulation Monte Carlo algorithm for simulating noncontinuum gas flow", *Phys. Fluid.*, **21**, 017103.

Bird, G.A. (2013), *The DSMC Method, Version 1.1*, Amazon, ISBS 9781492112907, Charleston, USA.

Collins, F.G. and Knox, E.C. (1994), "Parameters of nocilla gas/surface interaction model from measured acommodation coefficients", *AIAA J.*, **32** (4), pp 765-773.

Gallis, M.A., Torczynski, J.R., Rader, D.J. and Bird, G.A. (2009), "Convergence behavior of a new DSMC algorithm", *J. Comput. Phys.* **228**, 4532-4548.

Gupta, R.N., Yos, J.M. and Thompson, R.A. (1989), *A Review of Reaction Rates and Thermodynamic Transport Properties for an 11-Species Air Model for Chemical and Thermal Non-Equilibrium Calculations to 30,000 K*, NASA TM 101528.

Knechtel, E.D. and Pitts, W.C. (1973), "Normal and tangential momentum accommodation for Earth satellite conditions", *Acta Astronautica*, **18**(3), 171-184.

Lord, R.G. (1991), "Some extensions to the Cercignani-Lampis gas- surface. scattering kernel", *Phys. Fluids* **A3**(4), 706-710.

Nocilla, S. (1962), "The surface re-emission law in free molecule flow", *Proceedings of the 3rd International Symposium on Rarefied Gas Dynamics*, Paris, France, June.

Moss J.N. (1995), *Rarefied Flows of Planetary Entry Capsules*, Special course on "Capsule Aerothermodynamics", Rhode-Saint-Genèse, Belgium, AGARD-R-808, 95-129, May.

Schamberg, R. (1959a), *A New Analytical Representation of Surface Interaction for Hyper-thermal Free Molecule Flow*, Rand Corp., RM-2313, Santa Monica, CA, USA.

Schamberg, R. (1959b), *Analytic Representation of Surface Interaction for Free Molecular Flow with Application to Drag of Various Bodies, Aerodynamics of the Upper Atmosphere*, Rand Corp., R-339, Santa Monica, CA, USA.

Shen, C. (2005), *Rarefied Gas Dynamic: Fundamentals, Simulations and Micro Flows*, Springer-Verlag, Berlin, Germany.

Zuppardi, G., Morsa, L., Savino, R., Sippel, M. and Schwanekamp, T. (2015), "Rarefied aerodynamic characteristics of aero-space-planes: a comparative study of two gas-surface interaction models", *Eur. J. Mech. B/Fluid..*, **53**, 37-47.

EC

Nomenclature

AoA	= angle of attack
C	= molecular thermal velocity
C_d, C_l, C_m	= drag, lift, longitudinal moment coefficients
C_p, C_f, C_h	= pressure, skin friction, heat flux coefficients
c	= airfoil chord and most probable molecular velocity
E	= aerodynamic efficiency ($E=C_l/C_d$) and molecule transitional energy
f	= fraction of molecules reflected specularly
h	= altitude
I_0	= Bessel function of zeroth order
Kn	= Knudsen number

k	= Boltzmann constant
L_x, L_y	= dimensions of computing region
M	= Mach number
m	= mass of a molecule
mcs	= mean collision separation
N	= number density
p	= pressure
Re	= Reynolds number
s	= curvilinear abscissa
T	= temperature
U, V, W	= components of thermal velocity along the x-, y- and z-axis
u, v, w	= components of velocity of a molecule along the x-, y- and z-axis
V_∞	= free stream velocity
$V_{\infty x}, V_{\infty y}, V_{\infty z}$	= components of the free stream velocity along the x-, y- and z-axis
α	= accommodation coefficient
$\alpha_{O2}, \alpha_{N2}, \alpha_O$	= molar fraction of oxygen, nitrogen and atomic oxygen
δ	= flap deflection
φ	= complementary to incidence angle ($\varphi=\pi/2-\vartheta$)
λ	= free molecule path
ϑ	= incidence angle
ρ	= density
τ	= shear stress

Subscripts and superscripts

E	= energy
g	= geometrical
i	= incident
n	= normal
r	= re-emitted
s	= slip
t	= tangential
w	= wall
∞	= free stream

Acronyms

CLL	= Cercignani-Lampis-Lord
DFA	= Maxwell Diffusive Fully Accommodated
DSMC	= Direct Simulation Monte Carlo
PSP	= Maxwell Partially SPecular
SPE	= Maxwell SPEcular